State-based Versus Time-based Estimation of the Gait Phase for Hip Exoskeletons in Steady and Transient Walking

Tian Ye[1], Ali Reza Manzoori[1], Auke Ijspeert[1] and Mohamed Bouri[1]

***Abstract*— The growing demand for online gait phase (GP) estimation, driven by advancements in exoskeletons and prostheses, has prompted numerous approaches in the literature. Some approaches explicitly use time, while others rely on state variables to estimate the GP. In this article, we study two novel GP estimation methods: a State-based Method (SM) which employs the phase portrait of the hip angle (similar to previous methods), but uses a stretching transformation to reduce the nonlinearity of the estimated GP; and a Time-based Method (TM) that utilizes feature recognition on the hip angle signal to update the estimated cadence twice per gait cycle. The methods were tested across various speeds and slopes, encompassing steady and transient walking conditions. The results demonstrated the ability of both methods to estimate the GP in a range of conditions. The TM outperformed the SM, exhibiting a root-mean-squared error below 3% compared to 8.5% for the SM. However, the TM exhibited diminished performance during speed transitions, whereas the SM performed consistently in steady and transient conditions. The SM displayed a better performance in inclined walking and demonstrated higher linearity at faster speeds. Through the assessment of these methods in diverse conditions, this study lays the groundwork for further advancements in GP estimation methods and their application in assistive controllers.**

I. INTRODUCTION

Among the various configurations of lower-limb exoskeletons for partial assistance in endurance augmentation applications, single-joint devices are more common. The targeted joint is usually either the hip [1] or the ankle [2], given the major contribution of these joints to positive power generation in gait [3]. Thanks to the more proximal location of the hip joint, hip exoskeletons have fewer constraints in terms of design and weight. Moreover, due to differences in muscle characteristics, the hip joint requires a higher metabolic cost to produce similar mechanical power compared to the ankle [4]. This fact further highlights the potential of hip exoskeletons for metabolic savings. In order to enable their users to utilize the assistance, proper synchronization with the Gait Cycle (GC) of the user is essential.

An independent variable is often used to synchronize actuation events in controllers designed specifically for walking [5]. This synchronization is usually time-based, which requires the detection of discrete events such as heel strike (HS) or toe off. The detected event can be used to trigger the playback of a pre-defined actuation signal [6]. To have a more granular control over the synchronization, however, the continuous Gait Phase (GP) can be calculated by normalizing the elapsed time since the detected event over the GC duration. This enables using torque profiles, which are predefined maps giving torques as a function of the GP. Control strategies based on such synchronization approaches have shown promise in reducing the metabolic cost of walking at constant speeds, when adapted with proper timing and sufficient power [2], [7]. To obtain the GP in this manner, the average GC duration is typically estimated as the mean of a moving window of recent GC durations [8], [9]. A consequence of this approach is the inherent dependence on past GCs and events, which can lead to errors in case of variations and irregularities in gait. In particular, time-based strategies can encounter difficulties in transient states such as changing gait speed and walking up or down a varying slope [5].

As an alternative, methods relying on the state variables of the system have been proposed. A state variable that changes monotonically over each GC, also known as a phase variable, can be used to estimate the GP. Phase variables may have the potential to robustly parameterize the GC in real-time and better handle transient phases [10], since they mainly exploit the present state of the system. Selection of the phase variable is not trivial, since a perfect estimation of the GP necessitates linearity with respect to time, in addition to strict monotonicity.

The neuroscience literature indicates that muscle afferents of the hip joint are important for modulating gait even at the more distal joints in mammalian locomotion [11]. This physiological role points to potential of the hip joint angle and its dependent variables as candidate phase variables. However, the direct mapping from the hip joint angle to the GP loses uniqueness over the full GC, since its trajectory is only piecewise-monotonic. To resolve this problem, Phase Portraits (PPs) can be utilized, which also incorporate the time derivative of a state variable. By including information regarding the value and the rate of change of the state variable, the polar angle of the PP can thus create a unique mapping over the entire GC.

State-based methods using the polar angle of the PP have been shown to robustly represent the phase of human gait during non-steady walking conditions [10] [12]. In previous work, Villareal and Gregg [12] compared three portrait-based phase variables in terms of their ability to parameterize the kinematics under normal and perturbed walking. The phase variable calculated from the PP of the thigh angle versus its integral was shown to be a better alternative for real-time

*AM received funding from the European Union's Horizon 2020 research and innovation programme under the Marie Sklodowska-Curie Grant Agreement No. 754354.

[1]All authors are with the Biorobotics Laboratory (BioRob) of EPFL, 1015 Lausanne, Switzerland. {ali.manzoori, tian.ye, auke.ijspeert, mohamed.bouri}@epfl.ch

control applications to parameterize the GC. However, the angle profiles often contain a DC offset component, which leads to a drift in the integral. The DC offset itself can also shift the center of the portrait away from the origin. In addition, the angle trajectories are not perfectly sinusoidal, resulting in oblateness of the PPs. Shifting and scaling of the coordinates have been used to deal with the offset and oblateness, respectively [13] but the shape of the obtained PPs were still elliptical.

In another study, we proposed applying a linear transformation to the PP to reduce its ellipticity, which led to improvements in the accuracy of the GP estimation [14]. However, the estimation quality was only tested in steady walking and at one speed, and two other phase-portrait-based methods were used as controls. In this article, we investigate the performance of this novel state-based method in a variety of steady and transient walking conditions, and compare it to a new time-based approach capable of adapting to transient states. Both methods rely on the hip joint angle for synchronization; the state-based method by constructing a PP, and the time-based method by detecting events to estimate the GC duration. Inspired by the advantages of using the integral of signals observed in past studies [12], we use the first and second time integrals of the hip angle in our methods. The GP estimation performance is tested in walking at a variety of speeds and inclinations, and also during the transition phases between them. We hypothesized that the time-based method would provide a more accurate and linear estimation, whereas the state-based method would perform better in transition phases.

II. METHODS

A. GP Estimation

1) State-based Method (SM): In a dynamical system, the standard PP of a state variable x is formed by plotting the variable versus its time derivative, $\dot{x}$. In our state-based method, we construct the PP from the first- and second-order time integrals of the hip flexion/extension angle, θ_h (henceforth "hip angle"). To ensure centering of the PP around the origin, each integration is followed by a high-pass filter to remove the integration drift. Then, similar to previous works, a scaling factor is used to obtain similar ranges for x and $\dot{x}$, calculated as:

$$\alpha = \frac{x_{Max} - x_{min}}{\dot{x}_{Max} - \dot{x}_{min}} \tag{1}$$

where x_{Max} and $\dot{x}_{Max}$ are the upper bounds of x and $\dot{x}$ respectively, and x_{min} and $\dot{x}_{min}$ are their lower bounds. As shown in the previous work [14], the PP generated using this procedure has a tilted elliptical shape that is stretched along the main diagonal, resulting in nonlinearity of the GP estimation. A stretching transformation along the anti-diagonal is therefore introduced to mitigate this effect, using a 2D transformation matrix T as in:

$$\begin{pmatrix} x_T \\ \dot{x}_T \end{pmatrix} = T \begin{pmatrix} x \\ \dot{x} \end{pmatrix} \tag{2}$$

where the subscript $_T$ denotes the final PP coordinates after the transformation. The following generalized transformation matrix was used for stretching:

$$T = \begin{bmatrix} \frac{1+k}{2} & \frac{1-k}{2} \\ \frac{1-k}{2} & \frac{1+k}{2} \end{bmatrix} \tag{3}$$

Where k controls the degree of expansion and contraction. The value of k in this study was determined as 2.5 through a pilot experiment involving one subject under conditions matching the final protocol, where k was manually adjusted to increase circularity of the PPs.

Finally, the polar angle of the PP (ϕ) is given by:

$$\phi(t) = \text{atan2}(x_T(t), \alpha\ \dot{x}_T(t)) \tag{4}$$

The GP (denoted by p_{GC}) is then obtained by calculating the difference between the current value of the polar angle and its value at the moment of HS, ϕ_{HS}, and normalizing to get a percentage:

$$p_{GC}(t) = \frac{|\phi(t) - \phi_{HS}|}{2\pi} \times 100\% \tag{5}$$

This method is summarized in Fig. 1A.

2) Time-based Method (TM): In this method, we use feature recognition of the hip angle signal to regularly update the estimated duration of the GC. The estimation exploits the sine-like shape of the hip angle trajectory, and works by detecting the peaks and troughs of the signal in each GC, and calculating the time duration between two consecutive peaks or troughs. In order to facilitate the real-time feature detection and avoid errors due to short-term oscillations, the second-order time integral of θ_h is used instead of the angle itself, similar to the SM. The GC period estimation is thus updated according to one of the following:

$$T_{GC}[k] = t_{peak}[n] - t_{peak}[n-1] \tag{6}$$

$$T_{GC}[k] = t_{trough}[n] - t_{trough}[n-1] \tag{7}$$

where $T_{GC}[k]$ is the estimated GC period, and $t_{peak}[n]$ and $t_{trough}[n]$ denote the times of the peak and trough of the $\iint \theta_h dtdt$ signal in the n^{th} GC, respectively. Note that the index of the GC period (k) is different from the index of the GC itself (n), since the period is updated twice per GC, starting from the second GC. Therefore, k will be either $2(n-1)-1$ or $2(n-1)$. The GP is then calculated as:

$$p_{GC}(t) = \frac{t - t_{HS}[n]}{T_{GC}[k]} + p_o[k] \tag{8}$$

where $t_{HS}[n]$ is the time of the most recent HS event, and $p_o[k]$ is a phase offset value used to prevent discontinuities in the GP due to the discrete changes in T_{GC}. At each update of the period, p_o is therefore updated as follows:

$$p_o[k] = \left(\frac{t_u[n] - t_{HS}[n]}{T_{GC}[k-1]} + p_o[k-1] \right) - \frac{t_u[n] - t_{HS}[n]}{T_{GC}[k]} \tag{9}$$

where $t_u[n]$ is the time of the update (equal to either $t_{peak}[n]$ or $t_{trough}[n]$). This method is schematically illustrated in Fig. 1B.

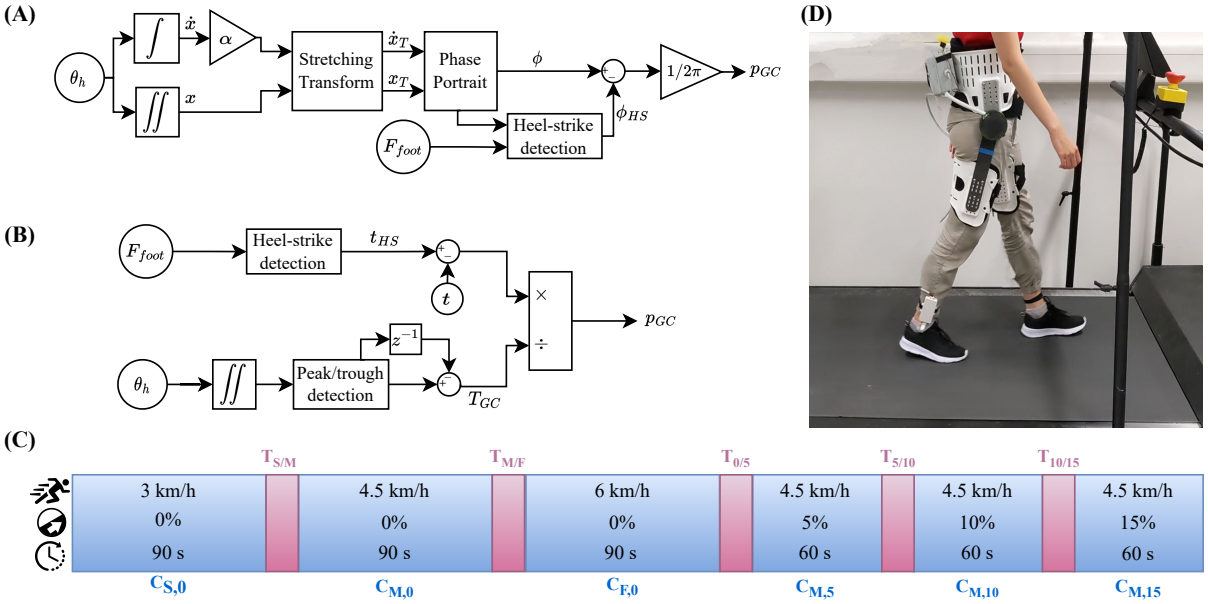

Fig. 1. (A) Schematic diagram of the state-based method. F_{Foot} denotes the ground reaction force signal sensed by the insole force sensors of the exoskeleton. (B) Schematic diagram of the time-based method. (C) The experimental conditions, including the speed, treadmill inclination, and duration of each condition. (D) The experimental setup, showing a subject walking on the treadmill while wearing the e-Walk V1 hip exoskeleton.

B. Experimental Setup and Protocol

A hip exoskeleton (e-Walk V1, Fig. 1D) is used for implementing and testing the GP estimation. The device has one active degree of freedom per leg (the flex./extension movement), in addition to the passive freedom of the abd./adduction movement due to the flexibility of the thigh segments in this direction. The actuators are only used in zero-torque mode in this study, in order to measure the hip angles. A pair of insole pressure sensors measure the foot contact information, which is used for HS detection and gait segmentation. An embedded computer (BeagleBone Black, BeagleBoard.org Foundation, USA) performs the data acquisition, logging, and the GP estimation at a frequency of $500\,\mathrm{Hz}$. The computer and batteries are mounted in a box on the back of the exoskeleton. The total weight of the exoskeleton is $5\,\mathrm{kg}$. A programmable treadmill with adjustable inclination (N-Mill, Forcelink B.V., the Netherlands) was used for all walking conditions.

Ten healthy young (aged 22–30, mean: 26.5 ± 2.7 years) adults (6 females, 4 males) were recruited for the experimental validation. The experiment protocol was reviewed and approved by the EPFL Human Research Ethics Committee. All subjects provided informed consent before participating in the experiments. In order to cover a wide range of walking conditions, the treadmill was programmed with a profile covering slow (S), medium (M), and fast (F) speeds (3, 4.5 and $6\,\mathrm{km/h}$, respectively) on the flat treadmill, and three inclinations (5, 10 and 15%) at the medium speed, as depicted in Fig. 1C, in the same chronological order. All speeds and inclinations were covered in one continuous walking session to also include the periods of transition between them. Hence, there were 11 conditions in total: 6 steady and 5 transition. The steady conditions are named $\mathrm{C_{X,\#}}$, where 'X' represents the speed (S/M/F) and '#' represents the inclination (0/5/10/15). The transition conditions are named $\mathrm{T_{A/B}}$, where 'A' and 'B' show the condition before and after the transition, respectively. For the speed transitions, only the speed labels appear in the transition name, and only the inclination numbers appear in the inclination transitions. The GP estimation using the two methods was performed in parallel on the embedded computer of the exoskeleton.

C. Data analysis

Since it was not possible to specify the duration of transition between speeds and slopes on the treadmill, the transition periods were detected in post-processing. For this purpose, the wavelet transform was applied to the hip angle to determine the dominant frequencies and the transition periods. This method allowed to determine both the time range and the duration of the transition periods. The data for each subject was thus divided into 11 separate sections (one per condition). Each section was then segmented into single GCs based on HSs detected from the insole pressure sensor signals. The segmentation was performed separately for each leg using the ipsilateral insole pressure data, but since the results were symmetric, only the left side was used in the analysis. The true GP for each GC was calculated by normalizing the time since HS over the real duration of that GC and used as the ground truth for error calculations. Also, the durations of the GCs were used to calculate the true GC frequencies. All data analysis was performed using MATLAB (Mathworks Inc., USA).

The following metrics were used for evaluating the GP estimation performance under each condition.

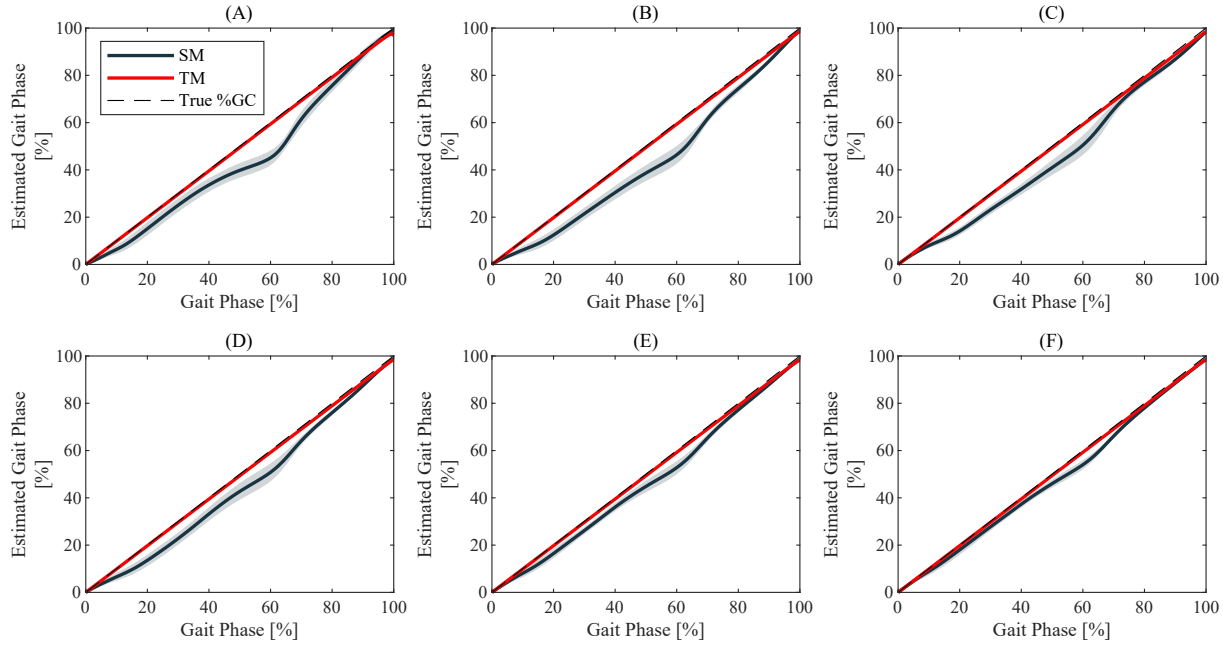

Fig. 2. Mean esitmated GP profiles estimated in the steady conditions: (A) $C_{S,0}$, (B) $C_{M,0}$, (C) $C_{F,0}$, (D) $C_{M,5}$, (E) $C_{M,10}$, (F) $C_{M,15}$. The shaded area around each line marks the standard deviation of the profile.

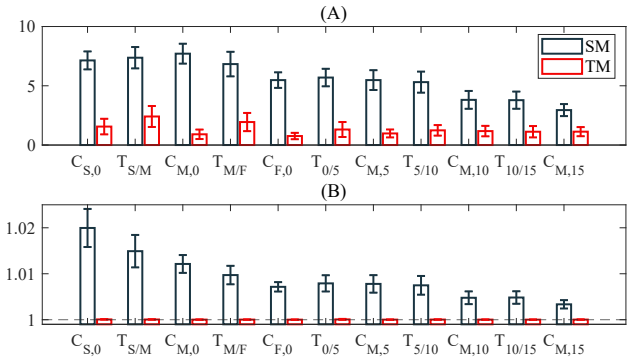

Fig. 3. Performance metrics of the GP estimation in different conditions: (A) RMS-E and (B) CLL.

1) Root-Mean-Square Error (RMS-E): This metric, which quantifies the accuracy of the estimation compared to the ground truth, was calculated as the RMS value of the error between the estimated and the true GP profiles in each stride, and then averaged over all subjects and strides.

2) Curve Length Linearity (CLL): This metric which characterizes the linearity of the estimated GP profiles, was defined as the ratio of the curve length of the profile to the distance between its starting and ending points. This score is always greater than or equal to 1, and values closer to 1 indicate a better linearity of the GP estimate, with a score of 1 meaning perfect linearity. It was calculated for each stride and was then averaged over all subjects and strides.

III. Results and Discussion

A. Overall Evaluation

The GP profiles estimated by the two methods averaged over each steady condition are presented in Fig. 2. In the transition conditions, given the small number of strides and their variability, averaging would not give a clear representation. Rather, the estimated GP curves over two transition periods for a representative subject are shown in Fig. 5. The performance metrics for all conditions are presented in Fig. 3 for a more quantitative comparison. Both the TM and SM show an acceptable estimation accuracy with average RMS errors under 3% and 8.5%, respectively (Fig. 3A), and the TM has a considerably better performance in all conditions. The TM also outperforms SM in terms of linearity, with a CLL score consistently near 1 (Fig. 3B). This is expected, since the GP profile estimated by the TM is piece-wise linear, with slopes that may slightly vary due to the updating of the GC duration.

B. Comparison across Steady Gaits

As can be seen in Fig. 2, the GP estimated by the TM in steady conditions mostly overlaps with true GP with a low deviation, which implies a high level of accuracy and linearity. During each steady condition, the GC frequency only varies within a small range and is therefore tracked well by the TM (Figs. 4A and 4C).

The GP estimated by the SM shows higher stride-to-stride variation compared to the TM. This is mostly caused by the variations in the shape of the PP (see Figs. 4B and 4D, for example), despite the use of the stretching transformation. This indicates that a constant transformation matrix cannot perfectly fit various subjects and walking conditions.

The SM shows better performance in terms of accuracy and linearity with increasing slope, in agreement with results we obtained in another study [14]. This improvement is likely attributable to a lighter impact at HS, which decreases knot-shaped local deformations of the PP occurring near heel-

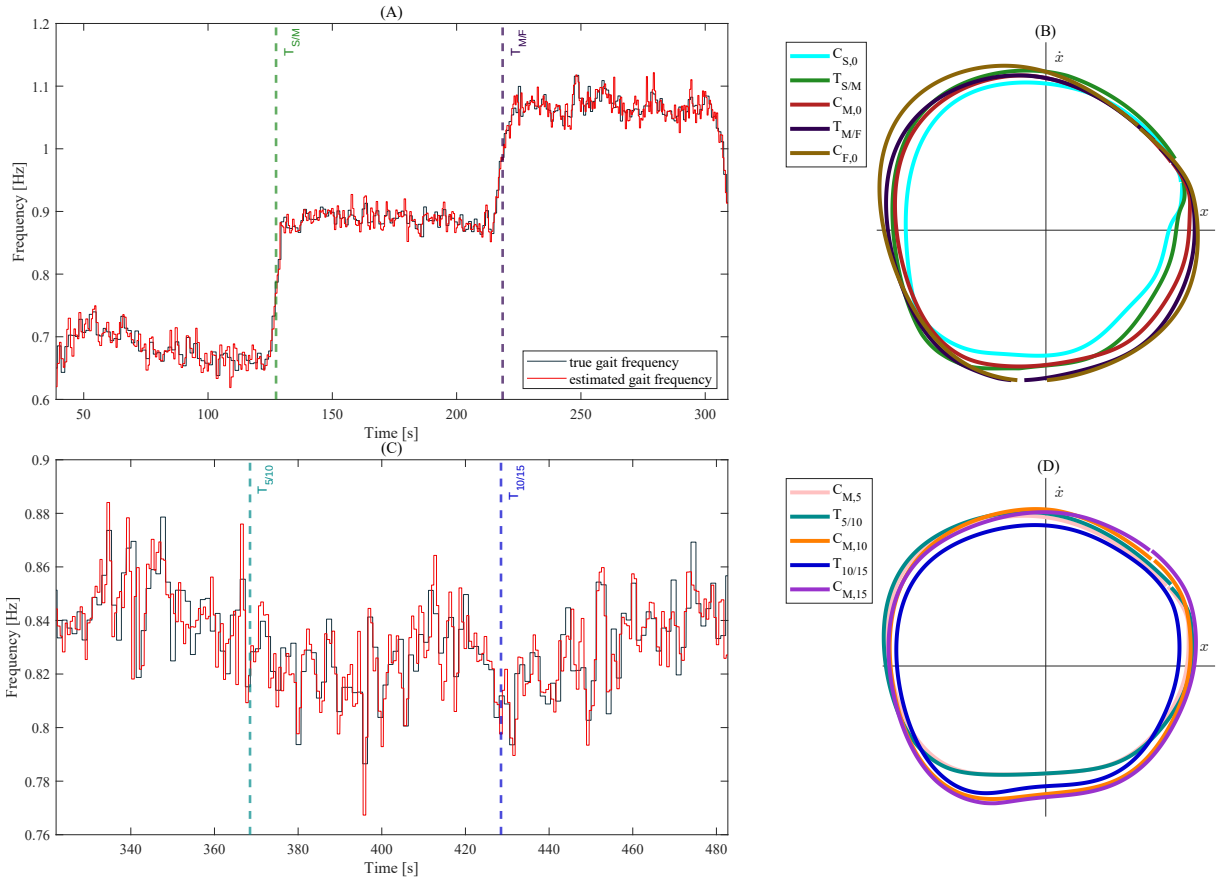

Fig. 4. Adaptation of the methods to different conditions for a representative subject: Actual versus estimated GC frequency of the TM in (A) flat and (C) slope; Evolution of average PPs across steady and transition conditions in (B) flat and (D) slope.

strike. An improvement in the linearity of the SM estimation is also observed with increasing speeds. Furthermore, the highest estimation accuracy of the SM in flat walking is observed in the fast speed. This improvement in linearity and performance is partly due to a more balanced stance/swing duration ratio at higher speeds [15]. Since geometrically stance and swing correspond to roughly equal angle ranges of the portrait, a more balanced duration ratio between them causes a more uniform rate of change of the polar angle over the GC. Furthermore, as can be observed in Fig. 4B, the portrait of $C_{S,0}$ is more irregular than $C_{F,0}$ around the border between the first and fourth quadrants. Speed seems to have a stronger influence on the SM portraits than slope, according to the variation between the portraits in Figs. 4B and 4D, also reflected in the linearity trends in Fig. 3B.

C. Comparison in Speed Transitions

Contrary to our hypothesis, the TM had a better performance even during speed transitions. Unlike conventional time-based approaches, the TM updates its GC duration estimation twice per stride without heavy dependence on past behavior, thus enhancing its reactivity in transient states. Nonetheless, the accuracy of the TM is more strongly affected during speed transitions as compared to the SM (Fig. 3A), due to the rapid changes in stride frequency as shown in Fig. 4A. Increasing cadence during the transition to higher speeds causes the HS to occur earlier and resets the GP estimated by the TM prematurely (Fig. 5A). However, this has no major impact on the linearity.

The SM is not significantly affected by speed changes, and its performance in each transition condition is consistent with the steady conditions before and after it (Fig. 3), as also reflected in the evolution of the PPs in Fig. 4B. A trend toward larger radius of the PP is also observed with increasing speeds, echoing previous observations in the literature [13].

D. Comparison in Slope Transitions

The TM outperformed the SM in slope transitions in terms of both metrics (Fig. 3). As observed in Fig. 4C, there are no significant and rapid changes in gait frequency during slope transitions. Therefore, the gait frequency tracking of the TM and thus its performance are not affected by slope transitions. The TM can thus maintain a consistently good performance (Fig. 3). Similar to the speed changes, the SM is not negatively affected by the changes in slope either. However, in slope transitions, its accuracy is closer to the steady condition before the transition (Fig. 3A). Opposed to the speed transition trends, the evolution of the PPs across different slopes does not show any significant trend (Fig. 4D).

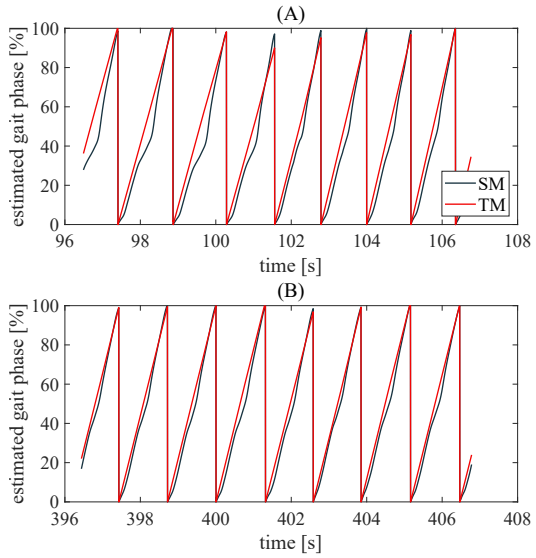

Fig. 5. Estimated GP profiles in two representative transient phases: (A) $T_{S/M}$ and (B) $T_{10/15}$.

E. Limitations and Future Work

In this work, a treadmill was used for both steady and transitory walking. Due to the quick transition of the treadmill between speeds and slopes, the number of transitory strides was low. Therefore, the assessment of the performance in transitions and the calculated metrics are less representative. Experiments in overground walking could facilitate a better assessment of the performances during transitions and provide more samples, in addition to yielding more realistic conditions representative of real-world behavior. The main shortcoming of the SM is its reliance on a constant transformation matrix, whilst the raw PPs evolve between subjects and conditions. An online adaptive transformation can thus improve its performance. Although the TM can track the GC frequency well overall, its performance declines during rapid transitions involving significant changes in cadence. This limitation can be mitigated by increasing the number of update events within a single GC (currently two), enhancing the sensitivity to changes in walking pattern.

IV. CONCLUSION

We proposed and tested two novel methods for GP estimation, using state-based and time-based approaches. Compared to previous state-based approaches, the SM was modified by stretching the PP to obtain a more circular shape. As an improvement to previous time-based approaches, the TM was modified to update of the GC duration more frequently, enabling faster reaction to transitions. Both methods showed an acceptable estimation performance in terms of accuracy and linearity. The TM had a better performance in all conditions, with RMS-E under 3% and CLL of 1, versus under 8.5% and 1.02 for the SM. During steady walking, the TM had a stable level of accuracy across different speeds and slopes. The SM, on the other hand, displayed a markedly higher accuracy and linearity at larger inclinations. Its linearity also improved with increasing speeds. Despite its better performance, the accuracy of the TM was negatively affected during the speed transitions, due to its dependence on the GC duration estimation. Slope transitions did not affect the TM. The SM was not affected during the transitions, showing a seamless shift between the performance of the steady states before and after the transition.

ACKNOWLEDGMENT

The authors would like to thank Sara Messara for her help in carrying out the experiments, and also Dr. Romain Baud and Dr. Olivier Pajot for their help in preparation of the hardware and software platforms.

REFERENCES

[1] J. Olivier, M. Bouri, A. Ortlieb, R. Clavel, and H. Bleuler, "A ball-screw driven motorized hip orthosis," Transaction on Control and Mechanical Systems, 2014.

[2] S. Galle, P. Malcolm, S. H. Collins, and D. De Clercq, "Reducing the metabolic cost of walking with an ankle exoskeleton: interaction between actuation timing and power," Journal of neuroengineering and rehabilitation, vol. 14, no. 1, pp. 1–16, 2017.

[3] D. A. Winter, Biomechanics and motor control of human movement. John Wiley & Sons, 2009.

[4] B. R. Umberger and J. Rubenson, "Understanding muscle energetics in locomotion: new modeling and experimental approaches," Exercise and sport sciences reviews, vol. 39, no. 2, pp. 59–67, 2011.

[5] M. R. Tucker, J. Olivier, A. Pagel, H. Bleuler, M. Bouri, O. Lambercy, J. d. R. Millán, R. Riener, H. Vallery, and R. Gassert, "Control strategies for active lower extremity prosthetics and orthotics: a review," Journal of neuroengineering and rehabilitation, vol. 12, no. 1, pp. 1–30, 2015.

[6] J. R. Koller, C. David Remy, and D. P. Ferris, "Comparing neural control and mechanically intrinsic control of powered ankle exoskeletons," in 2017 International Conference on Rehabilitation Robotics (ICORR), 2017, pp. 294–299.

[7] J. Zhang, P. Fiers, K. A. Witte, R. W. Jackson, K. L. Poggensee, C. G. Atkeson, and S. H. Collins, "Human-in-the-loop optimization of exoskeleton assistance during walking," Science, vol. 356, no. 6344, pp. 1280–1284, 2017.

[8] I. Kang, H. Hsu, and A. Young, "The effect of hip assistance levels on human energetic cost using robotic hip exoskeletons," IEEE Robotics and Automation Letters, vol. 4, no. 2, pp. 430–437, 2019.

[9] R. L. McGrath and F. Sergi, "Single-stride exposure to pulse torque assistance provided by a robotic exoskeleton at the hip and knee joints," in 2019 IEEE 16th International Conference on Rehabilitation Robotics (ICORR), 2019, pp. 874–879.

[10] D. J. Villarreal, H. A. Poonawala, and R. D. Gregg, "A robust parameterization of human gait patterns across phase-shifting perturbations," IEEE Transactions on Neural Systems and Rehabilitation Engineering, vol. 25, no. 3, pp. 265–278, 2017.

[11] S. Rossignol, R. Dubuc, and J.-P. Gossard, "Dynamic sensorimotor interactions in locomotion," Physiological reviews, vol. 86, no. 1, pp. 89–154, 2006.

[12] D. J. Villarreal and R. D. Gregg, "Unified phase variables of relative degree two for human locomotion," in 2016 38th Annual International Conference of the IEEE Engineering in Medicine and Biology Society (EMBC), 2016, pp. 6262–6267.

[13] D. Quintero, D. J. Lambert, D. J. Villarreal, and R. D. Gregg, "Real-time continuous gait phase and speed estimation from a single sensor," in 2017 IEEE Conference on Control Technology and Applications (CCTA), 2017, pp. 847–852.

[14] A. R. Manzoori, T. Ye, D. Malatesta, C. Lugaz, O. Pajot, A. Ijspeert, and M. Bouri, "Gait phase estimation in steady walking: A comparative study of methods based on the phase portrait of the hip angle," in 2023 International Conference on Rehabilitation Robotics (ICORR), 2023 (to appear).

[15] F. Hebenstreit, A. Leibold, S. Krinner, G. Welsch, M. Lochmann, and B. M. Eskofier, "Effect of walking speed on gait sub phase durations," Human Movement Science, vol. 43, pp. 118–124, Oct. 2015.